引用格式：CHEN Wenxuan, HE Min, CHEN Ping, et al. Polyvinyl Pyrrolidone Segment Length Dependent Perovskite Crystallization Kinetics and Electroluminescence Performance[J]. Acta Photonica Sinica, 2023, 52(8):0816001
陈文轩，何敏，陈平，等. 聚乙烯吡咯烷酮链段长度依赖的钙钛矿结晶动力学和电致发光研究[J]. 光子学报，2023，52(8)：0816001

聚乙烯吡咯烷酮链段长度依赖的钙钛矿结晶动力学和电致发光研究

陈文轩[2,3]，何敏[4]，陈平[4]，陈琪[1,3]

（1 中国科学技术大学 纳米技术与纳米仿生学院，合肥 230026）
（2 中国科学技术大学 纳米科学技术学院，苏州 215123）
（3 中国科学院苏州纳米技术与纳米仿生研究所 创新实验室 中科院纳米光子材料与器件重点实验室，苏州 215123）
（4 西南大学 物理科学与技术学院 微纳结构光电子学重庆市重点实验室，重庆 400715）

摘 要：基于低温溶液工艺的钙钛矿发光二极管由于低成本，高色纯度，宽色域等优势受到广泛关注。然而，在溶液结晶成膜过程中，钙钛矿晶粒无规形核、快速生长，导致薄膜存在大量的针孔和缺陷，严重影响器件性能。本文通过原位荧光和结构表征技术证实，聚乙烯吡咯烷酮(PVP)添加剂在特定的链段长度下，能优化调控钙钛矿结晶动力学，延缓晶粒生长速度，使得钙钛矿薄膜粗糙度由1.489 nm降低到0.954 nm，缺陷密度从1.55×10^{18} cm^{-3}降低至1.05×10^{18} cm^{-3}。相应地，薄膜荧光量子产率从16.9%提升到58.9%，器件外量子效率从8.55%提高到了18.00%。本文通过原位表征技术，全方位解析了添加剂分子结构对钙钛矿结晶动力学的调控机理，为添加剂分子的优化设计提供了直观依据。

关键词：钙钛矿发光二极管；结晶动力学；聚合物添加剂；链段长度；原位表征
中图分类号：TN312.8 **文献标识码**：A **doi**：10.3788/gzxb20235208.0816001

0 引言

钙钛矿材料拥有可溶液加工、成本低廉、发射光谱窄和波长可调等优势，在发光二极管中的应用前景被广泛看好[1-3]。然而，在溶液加工成膜过程中，钙钛矿晶核分布杂乱且生长速度过快，导致钙钛矿薄膜覆盖率低、粗糙度大、缺陷多，引起严重的漏电和非辐射复合，从而降低钙钛矿发光二极管(Perovskite Light Emitting Diodes，PeLEDs)效率[4-9]。

通常，在钙钛矿旋涂过程中滴加反溶剂(如乙酸乙酯，氯苯等)，能够迅速去除多余溶剂，并与前驱体形成中间相。再结合退火或负压处理等，中间相逐渐转变成钙钛矿相，可以得到致密的钙钛矿薄膜[10-12]。与此同时，在钙钛矿前驱体溶液中加入较大尺寸的有机阳离子(PEA^+，TEA^+等)，连续的铅卤八面体将被切割成周期性的量子阱结构，实现较大的激子结合能和快速的能量转移，从而提高薄膜荧光量子产率(Photoluminescence Quantum Yield，PLQY)和器件外量子效率(External Quantum Efficiency，EQE)。而通过结构和官能团设计调控大尺寸阳离子的插层动力学，还可以改善薄膜形貌[13-17]。当加入更大尺寸的聚合物时(如聚甲基丙烯酸甲酯，聚偏二氟乙烯，聚乙二醇等)，其链段无法进入钙钛矿晶格而主要充当结晶的“框架”，限制形核位点，抑制晶粒自由、过快生长，并填充晶界间隙，有助于进一步优化薄膜质量[18-20]。然而，

基金项目：科技部国家重点研发计划(No. 2021YFA1202802)，国家自然科学基金(Nos. 21875280，21991150，21991153，22022205)，中国科学院稳定支持基础研究领域青年团队计划(No. YSBR-054)，江苏省碳达峰碳中和科技创新专项资金项目(No. BE2022026)，重庆市自然科学基金(No. CSTB2022NSCQ-MSX0438)
第一作者：陈文轩，wxchen2022@sinano.ac.cn
通讯作者：陈琪，qchen2011@sinano.ac.cn；陈平，pingchen@swu.edu.cn
收稿日期：2023-02-18；**录用日期**：2023-03-29

聚合物尺寸、流动性和溶解度等随着链段长度增加不断变化，显著影响钙钛矿晶体生长过程。因此，系统研究聚合物链段长度对钙钛矿结晶动力学的调控规律，对于提高钙钛矿薄膜质量进而提升其电致发光性能具有重要意义。

本文选用了聚乙烯吡咯烷酮（Polyvinyl pyrrolidone，PVP）这种常见的聚合物，一方面通过调节不同的分子量控制碳链长度，结合原位荧光和XRD等表征手段研究链段长度对准二维钙钛矿$PEA_2Cs_2Pb_3Br_{10}$结晶动力学过程的调控机制；另一方面利用其具有路易斯碱性的羰基，钝化钙钛矿中的缺陷。

1 实验方法

1.1 实验材料及钙钛矿前驱体溶液配制

各种分子量的聚乙烯吡咯烷酮（PVP-3 kDa，10 kDa，30 kDa，58 kDa，130 kDa，>98%）和乙酸乙酯（EA，SafeDry，99.8%）从阿达玛斯购买。溴化铅（$PbBr_2$，>99.99%）、苯乙基溴化铵（PEABr，>99.5%）和氟化锂（LiF，>99%）从西安宝莱特光电科技有限公司购买。聚（N-乙烯咔唑）（PVK，99.99%，Mw≈1 100 000）和溴化铯（CsBr，>99.999%）从Alfa Aesar购买。二甲基亚砜（DMSO，GC，>99.9%）和氯苯（CB，GC，>99.9%）从阿拉丁购买。1，3，5-三（1-苯基-1H-苯并咪唑-2-基）苯（TPBi，>99.5%）从吉林奥莱德光电材料有限股份公司购买。所有购得材料均直接使用.

PEABr，CsBr，$PbBr_2$按0.67∶1.27∶1的化学计量比溶解在1 mL二甲基亚砜（DMSO）中，其中Pb^{2+}浓度为0.2 mol/L，并分别加入1 mg/mL的PVP-3 kDa，10 kDa，30 kDa，58 kDa，130 kDa。随后在50 ℃下搅拌过夜，使用前经0.22 μm的滤头过滤后备用。

1.2 器件制备过程

ITO玻璃衬底在使用前分别在玻璃清洗剂、去离子水、乙醇、丙酮和异丙醇中超声清洗20 min，经氮气吹干之后用氧等离子体处理10 min，随后转入氮气手套箱。首先，将PVK（CB，6 mg·mL^{-1}）以4 000 r·min^{-1} 60 s旋涂在ITO上之后150 ℃退火20 min；接着，以3 000 r·min^{-1} 120 s旋涂钙钛矿前驱体溶液，在第40 s滴加反溶剂EA，旋涂结束之后70 ℃，退火10 min；最后，在真空度<5×10^{-4} Pa时，用掩膜版依次蒸镀TPBi（0.1 nm·s^{-1} 50 nm）、LiF（0.01 nm·s^{-1} 2.5 nm）、Al（0.1 nm·s^{-1} 100 nm）层，得到有效面积为0.04 cm^{2}的器件。

1.3 测试与表征

紫外-可见吸收光谱使用赛默飞公司的紫外可见分光光度计（Biomate 160）测得。荧光光谱使用日立公司的F4600荧光光度计测得。PLQY使用广州犀谱光电科技有限公司的XPQY-EQE-adv测试系统测得，激发波长365 nm。薄膜形貌使用牛津仪器Asylum Research公司的原子力显微镜（Cypher S）测得。XRD使用Bruker公司的X射线衍射仪（D8-ADVANCE）测得。PeLEDs的电流密度-电压（J-V）曲线、亮度-电压（L-V）曲线、外量子效率-电流密度EQE-J曲线均使用广州犀谱光电科技有限公司XPQY-EQE-adv系统在氮气手套箱中测得。

2 结果与讨论

2.1 成膜过程

为了研究聚合物链长如何影响钙钛矿成膜，在钙钛矿前驱体溶液中加入分子量3 kDa，10 kDa，30 kDa，58 kDa，130 kDa的PVP，经优化后在前驱体中添加浓度为2 mg/mL，并在旋涂时进行了原位紫外光激发，其中第40 s滴加反溶剂。图1为0 s，45 s，50 s，55 s，65 s时各薄膜的荧光照片。在第45 s，未添加PVP的薄膜已经发射出较强荧光，而添加PVP的薄膜随链长增加荧光逐渐减弱，其中添加PVP-130 kDa的薄膜几乎看不到荧光。随着旋涂时间增加，各薄膜荧光逐渐增强。未添加PVP的薄膜在第50 s之后荧光强度不再明显增强。不同的是，添加PVP的薄膜随链长增加，荧光达到最强的时间逐渐延后，且最终的荧光强度逐渐降低。

进一步地，如图2（a）所示测试了薄膜经历不同旋涂时间的X射线衍射（X-Ray Diffraction，XRD），研究链长对于结晶速率的影响。对于未添加PVP的薄膜，在第45 s出现了较强的（202）衍射峰，随旋涂时间增加（202）衍射峰强度略有增加，并在第55 s后不再明显增加。而对于添加PVP的薄膜，在第45 s出现的（202）

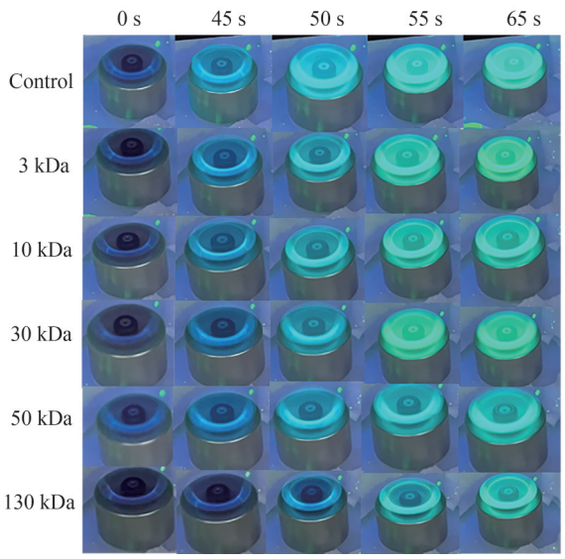

图1　在365 nm紫外光激发下，旋涂中不同时间点的钙钛矿薄膜

Fig.1　365 nm UV excited perovskite films at different time points during spin-coating

衍射峰强度随着链长增加而逐渐降低，其中添加PVP-58 kDa，130 kDa的薄膜衍射峰强度非常弱。此外，随着链长增大，(202)衍射峰强度随旋涂时间增加的速度逐渐变慢，并且最终的强度也逐渐减弱。如图2(b)所示，旋涂结束后各薄膜均有对应于$CsPbBr_3$ (101)和(202)晶面的2θ～15.2°和30.5°的衍射峰，表明前驱体均转变形成了钙钛矿。但是，添加PVP的薄膜的衍射峰强度随着链长逐渐降低。以(202)晶面的衍射峰为例，添加了PVP-3 kDa，10 kDa，30 kDa，58 kDa，130 kDa的薄膜的强度分别为未添加PVP薄膜的97.63%，91.79%，74.62%，71.14%和66.79%。

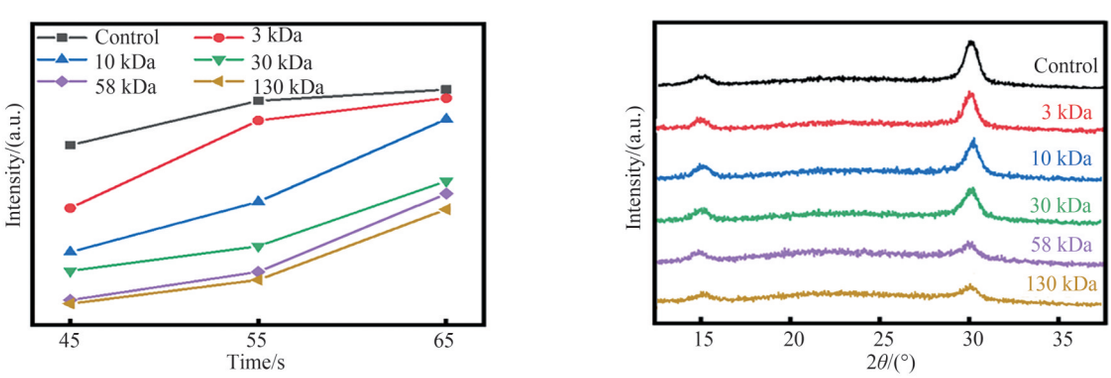

(a) Intensity changes of (202) peak at different time points during spin coating　(b) XRD diagram after spin-coating

图2　薄膜XRD测试

Fig.2　XRD tests of thin films

结合原位荧光和XRD数据能够说明，未添加PVP的薄膜在滴加完反溶剂后的中间相在短时间内迅速转变成钙钛矿相，之后结晶性不再明显变化。而添加PVP的薄膜在滴加完反溶剂后，PVP链段延缓了中间相向钙钛矿相的转变，结晶性随着旋涂时间增加而增强。但当PVP链长过长时，例如PVP-30 kDa，58 kDa，130 kDa，其较差的流动性和堆积的长链导致结钙钛矿晶过程被过分抑制，结晶速率过慢，结晶性明显减弱。

2.2　薄膜荧光吸收光谱和缺陷变化

钙钛矿结晶速率随PVP链长的变化，将会显著影响钙钛矿薄膜的光学性能。图3(a)为未添加PVP和添加PVP的薄膜的荧光光谱，可以看到荧光强度随PVP链长的增加逐渐上升，其中添加PVP-10 kDa的薄膜荧光强度最强。相对应地，薄膜的PLQY由未添加PVP的16.9%提升到添加PVP-10 kDa的58.9%(图3(b))。但是，当PVP链长进一步增加，荧光强度和PLQY逐渐降低。与此同时，PVP还引起了钙钛矿薄膜PL峰位的变化。随PVP链长增加，薄膜的PL峰位持续红移。无添加剂薄膜PL峰为507 nm，添加

PVP-3 kDa,10 kDa,30 kDa的薄膜PL峰位逐渐红移至508 nm,509 nm,510 nm。继续增加PVP链长,PL峰位保持不变,稳定在510 nm。为了理解PVP对薄膜荧光强度和峰位的影响,进一步做了紫外-可见吸收光谱测试(Ultraviolet-Visible Spectrum UV-Vis),如图3(c)所示。未添加PVP的薄膜,在403 nm,434 nm,465 nm波长处存在多个吸收峰,分别对应准二维钙钛矿n=1,2,3的低维相。添加PVP的薄膜,对应于n=1,2,3低维相的吸收峰被有效抑制。

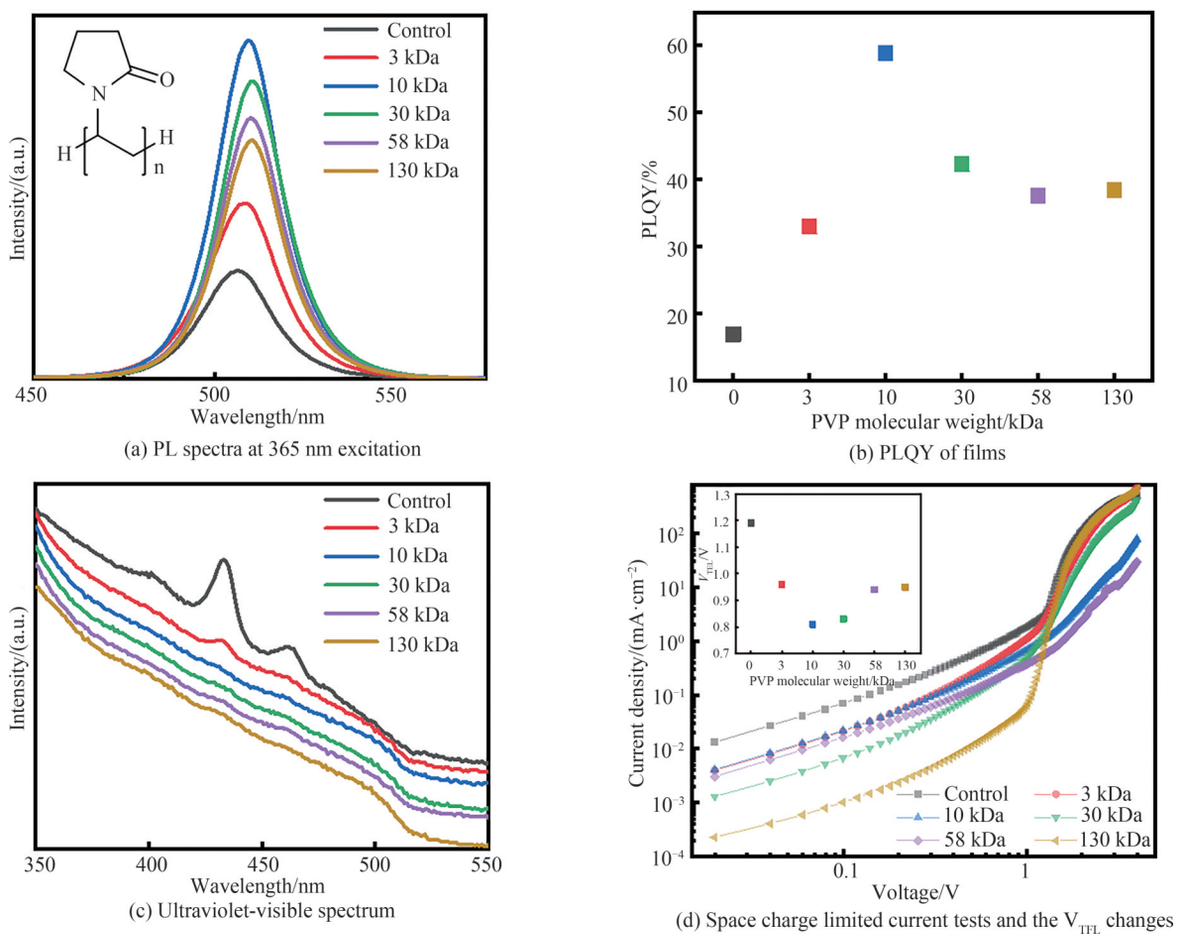

图3 薄膜荧光、紫外吸收和SCLC测试

Fig.3 Photoluminescence, ultraviolet-visible spectrum and SCLC tests

为了说明聚合物链长对钙钛矿薄膜缺陷密度的影响,通过空间电荷限制电流法(Space Charge Limited Current,SCLC)测量了钙钛矿薄膜在添加不同链长PVP后的缺陷填充电压(The Trap-filled Limiting Voltage V_{TFL})。图3(d)为结构为PVK/Perovskite/MoO_3/Ag单空穴器件的J-V曲线图和缺陷填充电压V_{TFL}的变化趋势。随着PVP添加剂链长的增大(3 kDa-10 kDa),其V_{TFL}由1.19 V降低到0.81 V;当PVP添加剂链长进一步增大(30 kDa-130 kDa),V_{TFL}又逐渐增加到0.95 V。通过缺陷密度计算公式$N=(2\ V_{TFL}\cdot\varepsilon_r\cdot\varepsilon_0)/(eL^2)$,其中$N$为缺陷密度,$\varepsilon_r$和$\varepsilon_0$分别为钙钛矿材料的介电常数与真空介电常数,$e$为单位电荷,$L$为钙钛矿薄膜的厚度,算得添加不同PVP后薄膜对应缺陷密度由control的1.55×10^{18} cm^{-3}分别变为1.25×10^{18}(3 kDa),1.05×10^{18}(10 kDa),1.08×10^{18}(30 kDa),1.22×10^{18}(58 kDa),1.24×10^{18} cm^{-3}(130 kDa),具有先减低后升高的趋势。这些数据表明,优化的PVP链长有效延缓钙钛矿结晶,抑制低维相生成,从而避免激子-声子耦合和激子转移迟滞,并且减少薄膜内部的缺陷态密度,获得更强的荧光[21-22]。同时,带隙较宽的低维相被抑制,转变成带隙较窄的三维钙钛矿,引起PL峰位红移。但是当PVP链长过长时将会抑制钙钛矿结晶,损害晶体质量,导致缺陷密度增大,降低薄膜荧光强度。

2.3 薄膜形貌

钙钛矿结晶速率随PVP链长的变化会影响钙钛矿薄膜形貌。图4是利用原子力显微镜测量的未添加

PVP和添加PVP的薄膜的形貌，未添加PVP的粗糙度为1.489 nm，可以看到存在低维相引起的零星小颗粒。而添加PVP-3 kDa，10 kDa，30 kDa，58 kDa，130 kDa的粗糙度分别为1.142 nm，0.954 nm，1.169 nm，3.624 nm，3.279 nm，呈现先下降后上升的趋势。可以看出，无添加剂时，钙钛矿结晶速率过快，形成较多低维相，增大薄膜粗糙度。对于添加PVP的薄膜，链长较短时（≤30 kDa），能够延缓结晶速度，抑制低维相生成，从而降低薄膜粗糙度。但是链长过长时（≥58 kDa），钙钛矿晶体生长受到抑制，晶粒分布不均匀，导致大量针孔和较高的粗糙度。

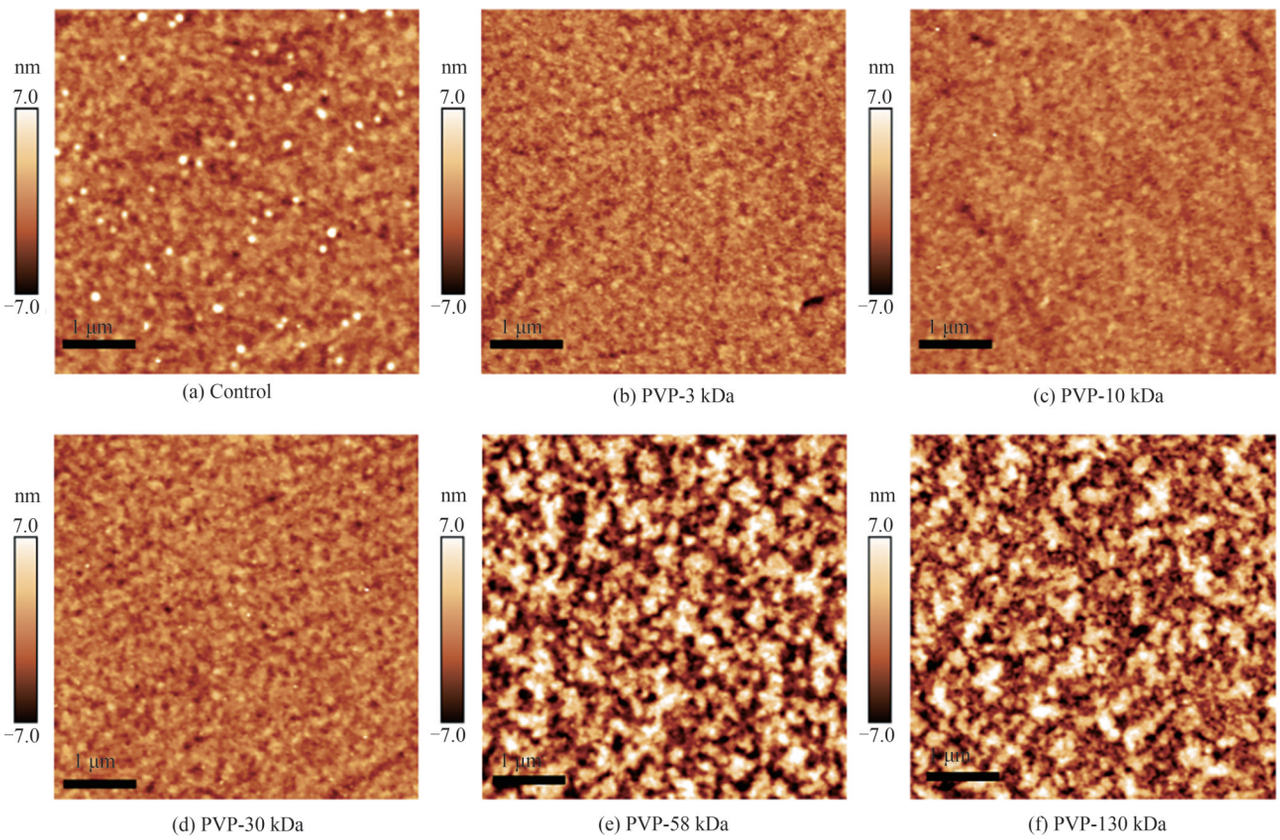

图4　薄膜AFM形貌图

Fig.4　AFM images of thin films

2.4　器件性能

通过优化PVP链长能够有效调控钙钛矿结晶动力学，同时增强薄膜荧光和改善薄膜形貌，有利于获得优越的电致发光性能。为此，本文详细优化了添加最优链长PVP-10 kDa前后的PeLED器件。图5(a)是器件结构为ITO/PVK/Perovskite/TPBi/LiF/Al的器件的*L*-*J*-*V*曲线。在添加PVP-10 kDa后，PeLED的电

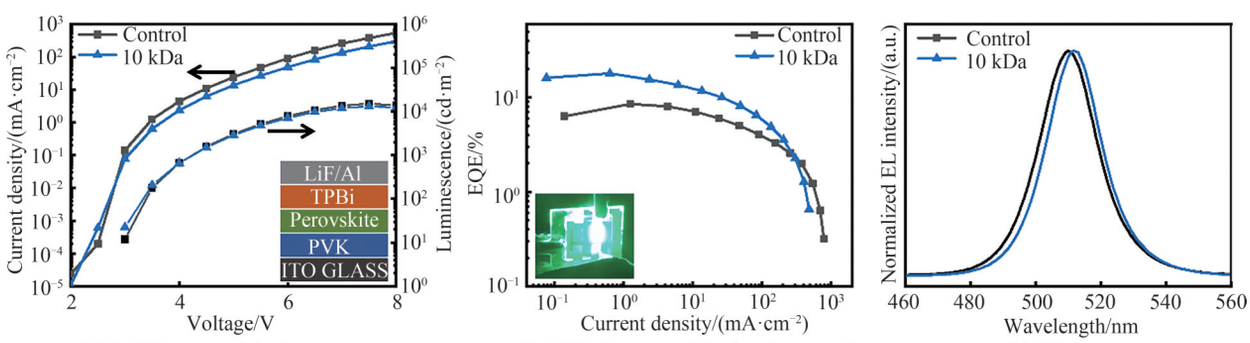

图5　器件性能对比

Fig.5　Device performance comparison

流密度明显下降，而亮度几乎保持不变，最大亮度分别为14 272 cd·m^{-2}和13 140 cd·m^{-2}。图5(b)是添加PVP-10 kDa前后的EQE-J曲线，可以看到添加PVP-10 kDa之后EQE显著提升，最大EQE从8.55%提升到了18.00%。图5(c)是添加PVP-10 kDa前后的EL光谱，可以看到峰位从510 nm红移至511 nm，这与荧光光谱的红移一致。

3 结论

综上所述，本文通过原位表征技术，证实了钙钛矿的结晶速率随着PVP链长的增加而逐渐降低，抑制了钙钛矿晶体的快速无规生长。在优化的PVP-10 kDa链长下，不仅获得了均匀致密的钙钛矿薄膜，而且缺陷密度降低，荧光强度显著增强。相应地，钙钛矿薄膜缺陷密度从1.55×10^{18} cm^{-3}降低至1.05×10^{18} cm^{-3}，PLQY从16.9%提升至58.9%，PeLED的EQE从8.55%提升到了18.00%。而当PVP链长较短时(≤3 kDa)，无法充分抑制晶粒的过快生长过程；当链长过长(≥30 kDa)，钙钛矿结晶性变差、缺陷增多，无法达到理想的优化效果。此工作全方位解析了聚合物链段依赖的钙钛矿结晶动力学过程，为钙钛矿成膜添加剂分子的优化设计提供了有益参考。

参考文献

[1] YU Binghai, YAN Caiman, RAO Longshi, et al. Study on fabrication technology and porperties of high quality perovskite quantum dots film[J]. Acta Photonica Sinica, 2018, 47(2): 0231001.
余彬海, 颜才满, 饶龙石, 等. 高质量钙钛矿量子点薄膜制备及性能研究[J]. 光子学报, 2018, 47(2): 0231001.

[2] ZOU Guangruixing, CHEN Ziming, LI Zhenchao, et al. Blue perovskite light-emitting diodes: opportunities and challenges [J]. Acta Physico-Chimica Sinica, 2021, 37(4): 91-115.
邹广锐兴, 陈梓铭, 黎振超, 等. 蓝光钙钛矿发光二极管:机遇与挑战[J]. 物理化学学报, 2021, 37(4): 91-115.

[3] LI Yan, LI Jinhang, XU Leimeng, et al. $CsPbI_3$ perovskite quantum dots: fine purification and highly efficient light-emitting diodes[J]. Acta Chimica Sinica, 2021, 79(1): 126-132.
李严, 李金航, 许蕾梦, 等. $CsPbI_3$钙钛矿量子点的精细纯化及其高效发光二极管的研究[J]. 化学学报, 2021, 79(1): 126-132.

[4] CHENG Tai, QIN Chuanjiang, WATANABE S, et al. Stoichiometry control for the tuning of grain passivation and domain distribution in green quasi-2D metal halide perovskite films and light-emitting diodes[J]. Advanced Functional Materials, 2020, 30(24): 2001816.

[5] CHEN Xuchan, GAO Feng, XU Bo, et al. Phosphine oxide additives for perovskite light-emitting diodes and solar cells [J]. Chem, 2023, 9(3): 562-575.

[6] JING Yuanzhi, SUN Changjiu, XU Jian, et al. Synthesis-on-substrate of quantum dot solids[J]. Nature, 2022, 612 (7941): 679-683.

[7] ZHANG Moyao, CHEN Qi, XUE Rongming, et al. Reconfiguration of interfacial energy band structure for high-performance inverted structure perovskite solar cells[J]. Nature Communications, 2019, 10(1): 4593-4602.

[8] XIANG Ting, LI Ting, PING Chen, et al. 12-Crown-4 ether assisted in-situ grown perovskite crystals for ambient stable light emitting diodes[J]. Nano Energy, 2022, 95: 10700.

[9] WANG Cheng, ZHANG Chi, LI Ruifeng, et al. Charge accumulation behavior in quantum dot light-emitting diodes[J]. Acta Physico-Chimica Sinica, 2022, 38(8): 57-63.
王成, 张弛, 黎瑞锋, 等. 量子点发光二极管中电荷累积行为[J]. 物理化学学报, 2022, 38(8): 57-63.

[10] JEON N, NOH J, SEOK S, et al. Solvent engineering for high-performance inorganic - organic hybrid perovskite solar cells[J]. Nature Materials, 2014, 13(9): 897-903.

[11] LIU Yang, CUI Jieyuan, JIN Yizheng, et al. Efficient blue light-emitting diodes based on quantum-confined bromide perovskite nanostructures [J]. Nature Photonics, 2019, 13(11): 760-766.

[12] CHEN Qi, CHEN Lei, YE Fengye, et al. Ag-incorporated organic-inorganic perovskite films and planar heterojunction solar cells[J]. Nano Letters, 2017, 17(5): 3231.

[13] ZHANG Li, SUN Changjiu, YUAN Mingjian, et al. High-performance quasi-2D perovskite light-emitting diodes: from materials to devices[J]. Light-Science & Applications, 2021, 10(1): 61-87.

[14] YU Danni, WEI Qi, NING Zhijun, et al. Quasi-2D bilayer surface passivation for high efficiency narrow bandgap perovskite solar cells[J]. Angewandte Chemie-International Edition, 2022, 134(20): e202202346.

[15] GUO Zhenyu, ZHOU Huanpin. Research progress of composition and structure design in perovskites for high performance light-emitting diodes[J]. Acta Chimica Sinica, 2021, 79(3): 223-237.
郭镇域, 周欢萍. 钙钛矿组分和结构设计及其发光二极管器件性能研究进展[J]. 化学学报, 2021, 79(3): 223-237.

[16] LIAN Xiaomei, ZUO Lijian, CHEN Bowen, et al. Light-induced beneficial ion accumulation for high-performance quasi-2D

perovskite solar cells[J]. Energy & Environmental Science, 2022, 15(6): 2499-2507.
[17] ZHANG Tao, GONG Simin, CHEN Ping, et al. Incorporation of a polyfluorinated acrylate additive for highperformance quasi-2D perovskite light-emitting diodes[J]. Acta Physico-Chimica Sinica, 2023, 39:2301024.
张涛, 龚思敏, 陈平, 等. 利用多氟丙烯酸酯添加剂提升准二维钙钛矿发光二极管性能[J]. 物理化学学报, 2023, 39: 2301024.
[18] BI Dongqin, YI Chenyi, LUO Jingshan, et al. Polymer-templated nucleation and crystal growth of perovskite films for solar cells with efficiency greater than 21%[J]. Nature Energy, 2016, 1(10): 16142-16147.
[19] FENG Wenjing, ZHAO Yaping, LIN Kebin, et al. Polymer-assisted crystal growth regulation and defect passivation for efficient perovskite light-emitting diodes[J]. Advanced Functional Materials, 2022, 32(34): 2203371.
[20] CHENG Lipeng, HUANG Jingsheng, SHEN Yang, et al. Efficient $CsPbBr_3$ perovskite light-emitting diodes enabled by synergetic morphology control[J]. Advanced Optical Materials, 2019, 7(4): 1801534.
[21] YUAN Shuai, WANG Zhaokui, XIAO Leixin, et al. Optimization of low-dimensional components of quasi-2D perovskite films for deep-blue light-emitting diodes[J]. Advanced Materials, 2019, 31(44): 1904319.
[22] SHEN Dongyang, REN Zhenwei, CHEN Yu, et al. Highly emissive quasi-2D perovskites enabled by a multifunctional molecule for bright light-emitting diodes[J]. ACS Applied Materials & Interfaces, 2022, 14(18): 21636-21644.

Polyvinyl Pyrrolidone Segment Length Dependent Perovskite Crystallization Kinetics and Electroluminescence Performance

CHEN Wenxuan[2,3], HE Min[4], CHEN Ping[4], CHEN Qi[1,3]
(1 *School of Nano-Tech and Nano-Bionics, University of Science and Technology of China, Hefei* 230026, *China*)
(2 *Nano Science and Technology Institute, University of Science and Technology of China, Suzhou* 215123, *China*)
(3 *CAS Key Laboratory of Nanophotonic Materials and Devices, i-Lab, Suzhou Institute of Nano-Tech and Nano-Bionics, Suzhou* 215123, *China*)
(4 *Chongqing key Laboratory of Micro&Nano Structure Optoelectronics, School of Physical Science and Technology, Southwest University, Chongqing* 400715, *China*)

Abstract: Solution-processed Perovskite Light-Emitting Diodes (PeLEDs) has drawn much attention due to their low cost, narrow emission spectra and wide color gamut. However, undesirable pinholes and defects of perovskite films impair device performance, which is attributed to the atactic nucleation and rapid crystallization during solution processing. In general, the antisolvent is added to the perovskite spin coating process to quickly remove excess solvent and form an intermediate phase. Combining with annealing treatment, mesophase gradually transforms into the perovskite phase and dense perovskite film can be obtained. At the same time, the larger organic cation (PEA+, TEA+, etc.) will cut continuous lead halide octahedron into the periodic quantum well structure to form quasi-two-dimensional perovskite which has a larger exciton binding energy and rapid energy transfer.

By adding the large polymers to the precursor, long segments cannot enter the perovskite lattice and act as the "framework" in the perovskite crystallization process, which can restrict nucleation sites, inhibit the rapid growth of grains and further optimize the film quality. However, the size, fluidity and solubility of the polymer change with the increase of the segment length, which significantly affects the growth of perovskite crystals. Therefore, it is crucial to systematically study the regulation law of polymer segment length on the crystallization kinetics of perovskite to improve the quality of perovskite thin films and thus promote the electroluminescence properties.

Polyvinyl Pyrrolidone (PVP), a common non-ionic polymer, its structure is relatively simple and carbon segment length can be accurately controlled by molecular weight. Moreover, PVP contains a carbonyl group, which can effectively passivate the defects in perovskite. In this work, perovskite crystallization kinetics has been tuned by the incorporation of Polyvinyl Pyrrolidone (PVP) with different segment length. Based on in-situ photoluminescence and X-Ray Diffraction (XRD) spectra, it showed that perovskite crystallization rate is retarded to inhibit small n phase formation by increasing the PVP segment length, which played an important role in determining perovskite film quality, such as crystallinity, charge carrier recombination and roughness, etc. After different segment PVP was added to

the precursors, the absorption peaks at 403 nm (n=1), 434 nm (n=2) and 465 nm (n=3) in the Ultraviolet-Visible Spectrum of the quasi-two-dimensional perovskite low-dimensional phase are significantly inhibited, which are considered adverse to Photoluminescence performance. According to space charge limited current tests, compared with films without additives, the defect density of the films decreased significantly after adding different segment PVP, reaching the minimum at PVP-10 kDa. And with the segment length continuing to increase (>10 kDa), the defect density will increase slightly. The short PVP segment (≤3 kDa) was not effective on adjusting the crystallization rate, resulting in minor improvement in roughness and photoluminescence quantum yield (PLQY) of the perovskite film. While the too-long PVP segment (≥30 kDa) inhibited crystallization, leading to high roughness, low crystallinity and deteriorated PLQY of the perovskite film. 1

With the suitable PVP segment length (~10 kDa), the perovskite crystallization kinetics can be optimized, which exhibited decreased roughness from 1.489 nm to 0.954 nm, decreased defect density from 1.55×10^{18} cm^{-3} to 1.05×10^{18} cm^{-3}, improved PLQY from 16.9% to 58.9%. Combined with superior morphology and PLQY of the perovskite films with PVP-10 kDa, it is promising to achieve a high electroluminescence performance. The PeLEDs before and after incorporation of PVP-10 kDa were prepared with a stacking structure ITO/ PVK/Perovskite/TPBi/LiF/Al. Compared with the control devices, the PVP-10 kDa devices showed little change in luminance but significantly reduced current density, which benefited improved maximum external quantum efficiency (EQE) from 8.55% to 18.00%. This work systematically investigated polymer segment length dependent perovskite crystallization and electroluminescence performance, which provides a guideline to design polymer additives to further promote the development of PeLEDs.

Key words: Perovskite light emitting diodes; Crystallization kinetics; Polymer additives; Segment length; In situ characterization

OCIS Codes: 160.4670; 310.3840; 310.6188; 310.6845

Foundation item: The Ministry of Science and Technology of China (No. 2021YFA1202802), the National Natural Science Foundation of China (Nos. 21875280, 21991150, 21991153, 22022205), the CAS Project for Young Scientists in Basic Research (No. YSBR-054), the Special Foundation for Carbon Peak Neutralization Technology Innovation Program of Jiangsu Province (No. BE2022026), the Fundamental Research Funds for the Natural Science Foundation Project of Chongqing (No. CSTB2022NSCQ-MSX0438)